

3D Ultrasound Imaging of Scoliosis with Force Sensitive Robotic Scanning

Maria Victorova, David Navarro-Alarcon and Yong-Ping Zheng

Abstract—The motivation of this work is to develop a robotic system for improving the 3D ultrasound assessment of scoliosis with the Scolioscan machine. The proposed automated approach can liberate sonographers from manipulating the probe over patient’s spine (this repetitive and tiring task may cause them musculoskeletal complications). The robotic system has the potential to enhance the imaging quality during scanning by ensuring a good acoustic coupling between the probe and tissues. This is done by exploiting force feedback so as to regulate the applied force during the manipulation task. An experimental study is presented to validate the feasibility of the proposed robotic scanning approach.

I. INTRODUCTION

Scoliosis refers to the spinal deformity along the coronal plane (yet it may involve deformities along other planes, e.g. sagittal and transverse). The gold standard for scoliosis assessment is based on X-ray imaging, which exposes patients to harmful radiation (repetitive use of this type of assessment may induce cancer in kids). Adolescent Idiopathic Scoliosis (AIS) is the most prevalent form of scoliosis affecting 2-3% of the population. It is often diagnosed during the pubertal growth spurt between 10-14 years of age [1].

To cope with the above mentioned problems, a new hazardless system (named as Scolioscan) for scoliosis assessment was recently developed [2]. This system uses ultrasound imaging, therefore, it does not expose the patient to harmful radiation coming from X-rays. This scanning system has several shortcomings. Firstly, the human operator needs to manually position the probe during the ultrasound examination, which might affect the repeatability of scanning. It has been demonstrated that robotic manipulation of the probe can improve the accuracy of 3D ultrasound image [3], [4]. Secondly, since the scoliosis patients may have different degrees of spinal deformity, their back’s surface is uneven which makes the operator to apply significantly higher forces during scanning (compared with the examination of other organs). Thirdly, as the operator needs to scan patient’s spine vertically during typical scoliosis assessments (which contrasts with horizontal scanning for other types of assessments), it may lead to potential muscle fatigue.

By using robotic manipulators to automate the 3D ultrasound assessment for scoliosis, the repeatability of procedure can considerably be improved. Also, the operator can be better protected from potential musculoskeletal disorders by avoiding uncomfortable postures and applying large forces.

The authors are with The Hong Kong Polytechnic University, Hong Kong email: maria.victorova@connect.polyu.hk
This work is supported in part by the HKPolyU under grant H-ZG4W, in part by the RGC under GRF grant 14203917.

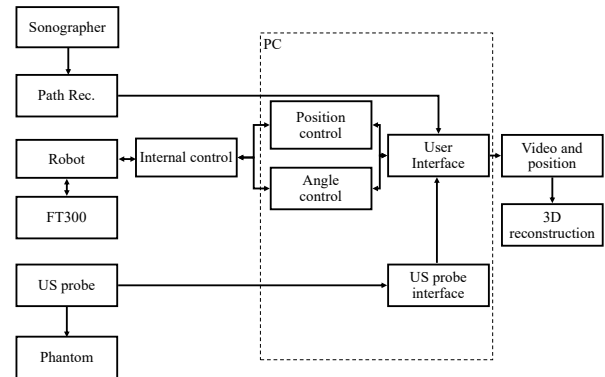


Fig. 1. The system block diagram of robotic system for 3D ultrasound assessment of scoliosis.

The idea of conducting ultrasound examinations with robots has been reported before, with the first solid project in this field conducted in 1990’s [5]. Currently, ultrasound robotic systems are used in many different medical areas, see e.g. [5]–[10]. However, to the best of the author’s knowledge, robots for spine examination have not been reported yet.

The aim of this work is to develop an ultrasound-based robotic system for the assessment of scoliosis. The system uses hybrid force/position control methods for manipulating the probe over body surfaces with different contour and stiffness. This robotic system can effectively automate the tiring probe manipulation task, while improving the task accuracy.

II. ROBOTIC SYSTEM

The major components of the new system are displayed in block diagram shown in Fig. 1. The system uses a collaborative robot (UR3, Universal robot, Denmark), which is safe to work with human in the same environment. Robot manipulates the wireless ultrasound probe (Shenzhen Eieling Technology, China). The system uses force/torque sensor (FT300, Robotiq, Canada) for force control.

The sensor provides accurate measurements of the interaction forces, with a resolution of 0.1 N (more sensitive than the ± 3.5 N internal force measurements of UR3) and sampling rate 1000 Hz. The robot communicates via TCP/IP protocol with a PC (where the control algorithm is implemented) at a rate of 125 Hz. The US probe captures images with a frequency of 7.5 MHz and a depth of 10 cm. The control algorithm is written in Python using the python-urx library. Two spine phantoms with different tissue stiffness

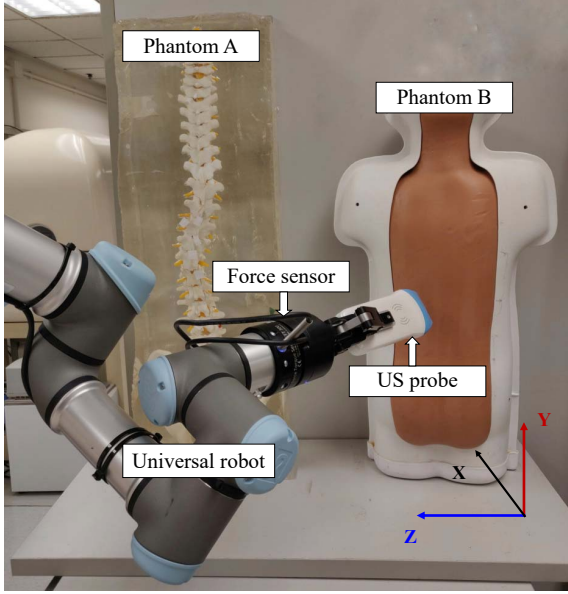


Fig. 2. Setup of robotic ultrasound scanning system.

are used for testing of system. Both spin phantoms are custom-made and have deformed spinal models embedded. The experimental setup is shown in Fig. 2.

III. CONTROL SYSTEM

A. Control tasks

In our application, the robot must be able to achieve the following control tasks:

- To maintain constant force against the spine during scanning.
- To avoid rotation of the probe when interacting with the tissues.
- To ensure acoustic coupling.
- To maintain the spine centred in the image.

The force is required to be constant for improving the patient's comfort and for avoiding excessive pressure, which might deform the observed anatomy. Ensuring acoustic coupling is crucial for ultrasound scanning procedures, otherwise the air between the tissue surface and the US probe would affect the propagation of acoustic ultrasound wave and an image cannot be formed. For the purpose of maintaining acoustic coupling, it is necessary to make real-time adjustments of angular alignment for the probe to be sufficiently tight to the surface of the phantom.

The position vector of the central point of the probe surface is $p = (x \ y \ z \ r_x \ r_y \ r_z)^T$. We use the measurements from the FT300 sensor, which are given in the form of the force screw $F = (f_x \ f_y \ f_z \ m_x \ m_y \ m_z)^T$, to perform real-time force regulation. For the current setup, the force coordinate pointing towards the phantom surface is f_x (to simplify notation, from now on, we shall denote this coordinate as $f = f_x$).

B. Force regulation

In this section we present the method to regulate the force in x-axis direction. Here the Hooke's law is used to relate the controllable motion variables (i.e. the robot positions/velocities) and the measurable force signal. Such mathematical model results in a linear relationship between forces and displacements. This common model has been used in other ultrasound robotic systems, see e.g. [11]. The general representation of this model (for the x-axis) is given as follows:

$$f = k\Delta x \quad (1)$$

where $k > 0$ denotes the (constant) stiffness gain of the phantom, and Δx represents the robot's relative displacements in x-axis direction.

The rate of change of the force values can be obtained by time differentiating f as:

$$\dot{f} = kv_x \quad (2)$$

In our system, the robot is driven by velocity commands that are fed into servo-controller, the velocity screw is $v = (v_x \ v_y \ v_z \ \omega_x \ \omega_y \ \omega_z)^T$. To reach control objectives, it is important to know the difference between desired force f_d and the actual force measurement from the sensor; we denote this force error signal as $e = f - f_d$. The purpose of the set-point force regulator is to minimize the error between measured and desired value. This can be achieved with a control action of following form:

$$v_x = -\lambda k^{-1}e = -Ce, \quad (3)$$

for $\lambda > 0$ and $C = k^{-1}\lambda$ as feedback control gains.

C. Position/moment control

For y-axis and z-axis we control the position of the robot with predefined scanning trajectory. In our current implementation, a human user defines the path along the y-z directions by manually driving the robot through a desired trajectory. These points are recorded, filtered, and then fed as target trajectory into the control algorithm. The main idea is to provide the robot with point-to-point incremental trajectories along the desired path.

The velocity commands for these axes are computed with the following feedback control law (3):

$$v_{y,z} = -C_{y,z}(p_{y,z} - p_{y,z}^*) \quad (4)$$

where $p_{y,z}$ denote the current y/z position of the robot, $p_{y,z}^*$ denotes the target positions taken from the recorded path, and $C_{y,z} > 0$ represents feedback gains.

The ultrasound probe has a distinctive rectangular shape whose orientation relative to the surface of the tissues needs to be well-aligned in order to ensure a stable contact and thus good acoustic coupling. To deal with this problem, the following moment-based control action is implemented

$$\omega_y = -C_{ry}(m_y - m_y^*) \quad (5)$$

for $C_{ry} > 0$ as the control gains, and m_y^* as the target moment which we set to 0.

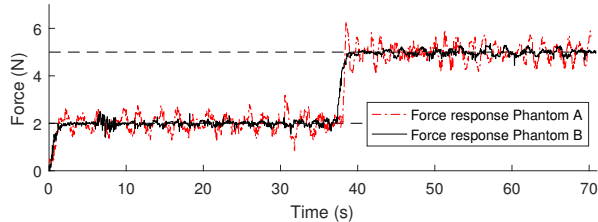


Fig. 3. Force step response for Phantom A with $C = 0.0005$ and Phantom B with $C = 0.0015$.

The final control uses the hybrid control [12]. The force together with the position are used as a feedback values for control of different axis, the method was named hybrid force/position control.

IV. EXPERIMENTAL RESULTS

In this section we present the experiments of the force regulation and the trajectory tracking (hybrid force/position control) to evaluate the proposed control method. The experimental setup is shown at the Fig. 2. Primarily, the stiffness gain k was calculated using the relation $\Delta f = k\Delta x$. The force output was measured for different Δx displacements of $\{0.5, 1, 1.5, 2\}$ mm with each Phantom. The computed mean stiffness for the Phantom A is $k_A = 589.5$ N/m and for Phantom B is $k_B = 194.5$ N/m.

Force step response. In this experiment, only the robot's x-axis was actively driven to achieve the target. The objective of this test was to evaluate the resulting force profile when controlling a discontinuous force target. According to the literature, the most common force range used in the US robotic examinations is 2–5 N. However, different tissue stiffness required to use different control parameters in the system. Fig. 3 shows the comparison of the force response for the Phantom A and Phantom B with control gains of $C = 0.0005$ and $C = 0.0015$, respectively.

Trajectory tracking. The procedure of this tracking experiment is illustrated in Fig. 4, which shows that the robot arrived to the initial location (a) and moved towards the phantom's surface (b) until it sensed a contact force (c). The system then applied a desired force reference, and started moving the probe along the prerecorded target trajectory (d). During these scanning motions, force and position data was collected. The results are shown in Fig. 5.

V. DISCUSSION

The proposed system uses a collaborative robot (cobot) instrumented with an external force sensor to perform the ultrasound scanning over the tissues (this feature improves the safety of this physically interactive task with humans). To automatically perform the scanning task, we proposed a solution to maintain the force applied onto the phantom tissues, and to adjust the appropriate rotation of the probe that ensures acoustic coupling. Note that the developed system uses of a wireless probe for US image capturing (this feature

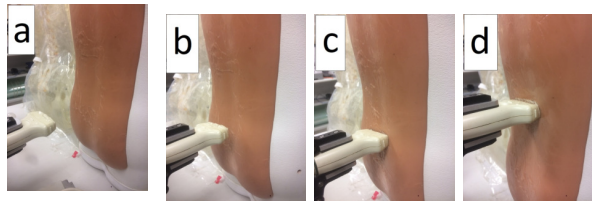


Fig. 4. Trajectory tracking experiment on Phantom B. a) initial position b) incremental move to the surface c) contact force sensed d) trajectory following with force control.

reduces the overall footprint as no bulky US machine is needed).

The stability of the robot was first examined with a zero force experiment to find an appropriate range of the control gains. The standard deviation was reduced by increasing the control gain C . Higher control gains result in faster reactions of the system to sudden force changes.

Nevertheless, the gain C was highly affected by the stiffness properties of the contact surface. Two phantom tissues (Phantom A and Phantom B) with different properties were scanned in this study. The stiffness ratio for the two environments is $n = k_A/k_B$. According to the data obtained during our experiments, the ratio is $n = 3$. Since $C = \lambda/k$, it can be expected that the control gain C_B for Phantom B would be three times greater than C_A for Phantom A.

The force controller for the “stiffer” Phantom A started to oscillate with a gain of $C = 0.001$ and reached a more accurate response with $C = 0.0005$, which was chosen for the final control implementation. For “softer” Phantom B, the control gain should be ideally 3 times larger, therefore, a value of $C = 0.0015$ was selected to achieve control objective. The final results of force control for two phantoms are presented in the Fig. 3.

In the last experiment, it is shown that force regulation during trajectory tracking has a satisfactory performance, and that the position deviation of the y and z axes is minimal. At the same time, the x-axis coordinate is corrected by the force control algorithm to ensure that the target force is applied onto the surface (see the x plot in Fig. 5). During the scanning of the spine phantom, US images were captured, and the Scolioscan software was used to process the images so as to reconstruct the 3D volumetric structure and to further form a coronal view image, see Fig. 6.

One limitation of the prototype is that the operator has not been completely excluded from the examination procedure yet. The current system requires the operator to first manually define the path for the robot to follow as an input trajectory. Another limitation is that the system cannot yet overcome a contour change on the surface of the phantom. The rectangular shape of the probe poses difficulties in sliding it along such contour, which might result in a loss of acoustic coupling with the surface of the Phantom. This problem could be dealt by using other types of probes or by means of orientation adjustments based on real-time force/moment measurements. We are currently working to overcome these issues.

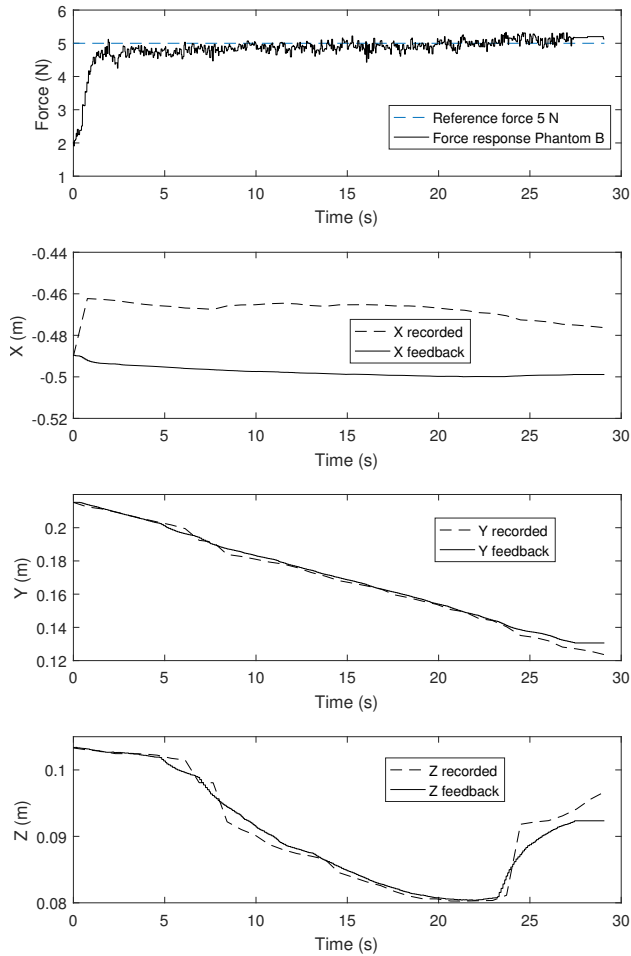


Fig. 5. Trajectory tracking results on Phantom B with $C = 0.002$.

VI. CONCLUSION

This study proposed a new robotic system for assessing scoliosis with ultrasound imaging. The robot is intended to be used alongside the Scolioscan system for reconstructing the 3D structure of the patient's spine. The feasibility of the system for performing the task was evaluated with two spine phantoms with different stiffness. Hybrid force/position control was implemented and evaluated experimentally. The difference of control parameters for the two different stiffness situations was demonstrated.

For future work, the quality of the scans will be estimated in order to modify the position of the probe so as to enhance the image acquisition. We plan to use image processing algorithms for tracking the spine at B-mode image to keep it centred while scanning and to control robot accordingly. This feature will enable the system to perform fully automated procedures that release human operators from manually performing these tasks. It is expected that the operators' role will be mostly supervisory.



Fig. 6. The coronal view ultrasound images of the Phantom B, reconstructed using Scolioscan software, at different depths and with different reconstruction parameters.

REFERENCES

- [1] D. B. M.A. Asher, "Adolescent idiopathic scoliosis: natural history and long term treatment effects." *Scoliosis*, vol. 1, no. 1, p. 2, 2006.
- [2] Y. Zheng et al., "A reliability and validity study for Scolioscan: a radiation-free scoliosis assessment system using 3D ultrasound imaging." *Scoliosis Spinal Disord.*, pp. 1–15, 2016.
- [3] K. Karadayi, Y. Kim, R. Managuli, and R. Managuli, "Three-Dimensional Ultrasound: From Acquisition to Visualization and from Algorithms to Systems," pp. 23–39, 2009.
- [4] R. W. Prager, U. Z. Ijaz, A. H. Gee, and G. M. Treece, "Three-dimensional ultrasound imaging," *Proceedings of the Institution of Mechanical Engineers, Part H: Journal of Engineering in Medicine*, vol. 224, no. 2, pp. 193–223, feb 2010.
- [5] S. E. Salcudean, W. H. Zhu, P. Abolmaesumi, S. Bachmann, and P. D. Lawrence, "A robot system for medical ultrasound Electromechanical desing," pp. 195–202, 1999.
- [6] K. Boman, J. Mona Olofsson, Forsberg, Boström, and Sven-Åke, "Remote-Controlled Robotic Arm for Real-Time Echocardiography: The Diagnostic Future for Patients in Rural Areas?" 2009.
- [7] R. Antonello, O. A. Daud, R. Oboe, and E. Grisan, "A telerobotic manipulation system for an immerse ultrasonic examination using haptic constraints," *IEEE International Symposium on Industrial Electronics*, pp. 1662–1667, 2012.
- [8] S. Virga, O. Zettinig, M. Esposito, K. Pfister, B. Frisch, T. Neff, N. Navab, and C. Hennersperger, "Automatic Force-Compliant Robotic Ultrasound Screening of Abdominal Aortic Aneurysms," 2016.
- [9] B. Wu and Q. Huang, "A Kinect-based automatic ultrasound scanning system," *ICARM 2016 - 2016 International Conference on Advanced Robotics and Mechatronics*, pp. 585–590, 2016.
- [10] K. Mathiassen, "An Ultrasound Robotic System Using the Commercial Robot UR5," *frontiers in Robotics and AI*, vol. 3, no. February, pp. 1–16, 2016.
- [11] P. Chatelain, A. Krupa, and K. Navab, "Confidence-Driven Control of an Ultrasound Probe," *2016 IEEE International Conference on Robotics and Automation*, 2017.
- [12] M. H. Raibert and J. J. Craig, "Hybrid Position/Force Control of Manipulators." *Journal of Dynamic Systems, Measurement, and Control*, vol. 126, no. 103(2), 1981.